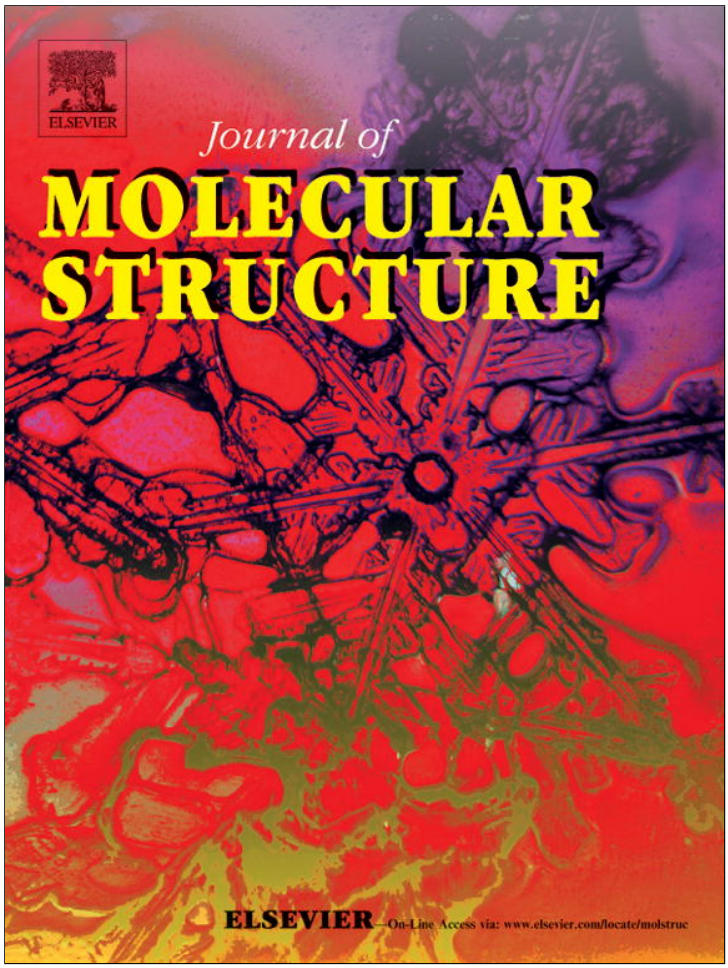

(This is a sample cover image for this issue. The actual cover is not yet available at this time.)

Journal of Molecular Structure 1028 (2012) 148–155

Contents lists available at SciVerse ScienceDirect

Journal of Molecular Structure

journal homepage: www.elsevier.com/locate/molstruc

Synthesis, characterization, crystal structure and thermal behavior of 4-Bromo-2-(((5-chloro-2-hydroxyphenyl)imino)methyl)phenol and its oxido-vanadium(V) complexes

S. Yousef Ebrahimipour [a], Joel T. Mague [b], Alireza Akbari [a], Reza Takjoo [c,*]

[a] Department of Chemistry, Payame Noor University (PNU), 19395-4697 Tehran, Iran
[b] Department of Chemistry, Tulane University, New Orleans, LA 70118, USA
[c] Department of Chemistry, School of Sciences, Ferdowsi University of Mashhad, Mashhad 91775-1436, Iran

HIGHLIGHTS

- New 2-[[(5-bromo-2-hydroxyphenyl)methylidene]amino]-4-chlorophenol is synthesized.
- The vanadium complexes were prepared and characterized by spectral and TGA techniques.
- The structures of compounds are determined by X-ray studies.
- The complexes show distorted square pyramidal and pentagonal bipyramid geometries.
- The ligand acts a zwitterionic form and complexes have octahedral and square pyramidal environment.

ARTICLE INFO

Article history:
Received 21 March 2012
Received in revised form 31 May 2012
Accepted 31 May 2012
Available online 23 June 2012

Keywords:
Vanadium complexes
ONO donor
TGA
Spectroscopy
Crystal structures

ABSTRACT

A new Schiff base ligand (ONO), 4-Bromo-2-(((5-chloro-2-hydroxyphenyl)imino)methyl)phenol and its vanadium(V) complexes [VO(L)(MeO)(MeOH)] **1**, $[VO(L)(EtO)]_2$ **2**, [VO(L)(2-BuO)] **3**, were prepared and characterized by elemental analyses, FT-IR, UV–Vis, ^{1}H NMR and TGA techniques. The structures of the free ligand and all complexes have been determined by X-ray diffraction. The ligand exists in a zwitterionic form while **1** has the metal in a distorted octahedral environment. Both **2** and **3** display distorted square pyramidal coordination for the metal with the former existing as a dimer while the latter is monomeric although showing a weak V—O interaction with a neighboring molecule.

1. Introduction

Vanadium complexes are effective catalysts in organic and inorganic precursor processes (such as oxidation, hydrogenation, etc.) [1–3]. They play an important biological role in the structure of the haloperoxidases and vanadium-nitrogenases as well [4,5]. Enhancement of insulin function or having an activity similar to insulin (important for diabetes type I and II) and normalizing the liver enzymes are some of the biological activities of vanadium complexes [6,7] and their role in the reduction of blood cholesterol and triglycerides has increased interest in their structure and coordination chemistry [8]. Their use in anti-neoplastic (mostly due to the ability of vanadium to cause DNA cleavage) [9] and antimicrobial agents [10] has made them appealing for identification and research studies.

The two predominant forms of vanadium under physiological conditions are the vanadyl cation and the vanadate anion [11]. The toxicity of vanadyl compounds is less than the other species of vanadium such as vanadate [12]. The dominant form of vanadium in intracellular reactions is vanadyl; therefore, it plays an important role in metabolic activities [13]. Vanadate-to-vanadyl conversion in blood plasma takes place by reducing agents such as glutathione. These ions combine with the proteins of transferrin and albumin and enter into body tissues [14]. While inorganic vanadium salts have considerable toxicity and low activity in biological fields, vanadium complexes with organic ligands are of great interest due to their reduced toxicity and increased adsorption by tissues [15]. Recently, several oxido-vanadium Schiff base complexes have been reported with the most attention focused

* Corresponding author. Tel./fax: +98 511 8975457.
E-mail address: rezatakjoo@yahoo.com (R. Takjoo).

0022-2860/$ - see front matter © 2012 Elsevier B.V. All rights reserved.
http://dx.doi.org/10.1016/j.molstruc.2012.05.076

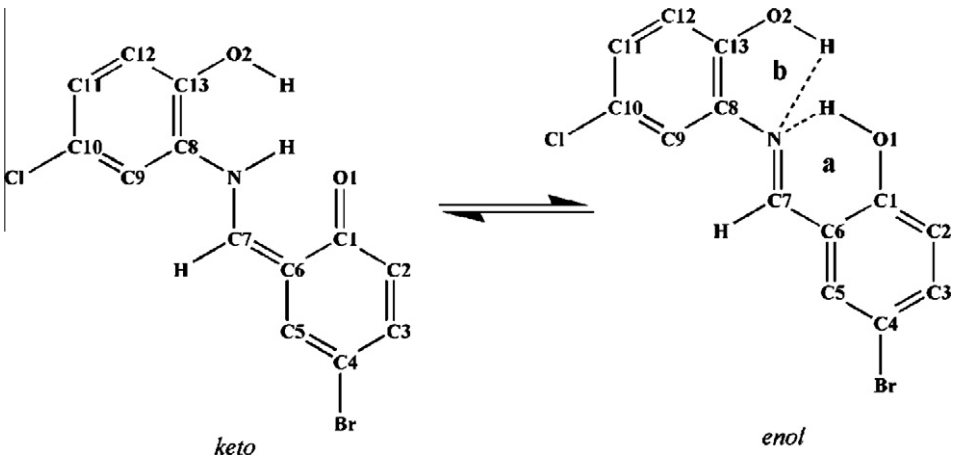

Scheme 1. The *keto-enol* forms of the free ligand (H_2L) (a: six-membered ring, b: five-membered ring).

on tri- and tetradentate ligands [16–18]. The most important tridentate ligands include those with NNS [19,20], NNO [21,22], ONO [23,24] and ONS [25,26] donor atoms.

This article focuses on the preparation and structural characterization of the new Schiff base ligand of the ONO type, 4-Bromo-2-(((5-chloro-2-hydroxyphenyl)imino)methyl)phenol and three oxido-vanadium complexes formed from it. In addition, we studied the effect of the ligand change on complex geometry.

2. Experimental

2.1. Materials and instrumentation

All chemicals were analytical grade and were used as received. Elemental analyses were carried out using a Thermo Finnigan Flash Elemental Analyzer 1112EA. The FT-IR spectra were recorded with a FT-IR 8400-SHIMADZU spectrophotometer. Conductance measurements were made by means of a Metrohm 712 Conductometer in DMSO. ^{1}H-NMR spectra were recorded at 25 °C with a Bruker BRX 100 AVANCE spectrometer. For referencing, known solvent (or residual solvent) signals were used. The electronic spectra were recorded in DMSO on a SHIMADZU model 2550 UV–Vis spectrophotometer. The TGA diagrams were recorded in a TGA-50 SHIMADZU instrument at a heating rate of 10 °C/min under air atmosphere over the temperature range of 20–850 °C. Diffraction data were measured using a Bruker Smart APEX CCD diffractometer. Atom labeling referred to in FT-IR and ^{1}H NMR peak assignments is outlined in Scheme 1.

2.2. Synthesis of 4-Bromo-2-(((5-chloro-2-hydroxyphenyl)imino)methyl)phenol (H_2L)

5-Bromo-2-hydroxybenzaldehyde (0.04 g, 0.2 mmol) in 5 ml ethanol was mixed with a 5 ml ethanolic solution of 2-amino-4-chlorophenol (0.03 g, 0.2 mmol). The mixture was refluxed on a water bath for 30 min. and after cooling the resulting red precipitate was separated by filtration, washed with cold ethanol and dried in a desiccator over anhydrous $CaCl_2$.

Block. red. Yield: 0.054 g, 82%. m.p.: 199 °C. Anal. Calc. for $C_{13}H_9BrClNO_2$ (326.57 g mol^{-1}): C, 47.81; H, 2.87; N, 4.29. Found: C, 47.78; H, 2.80; N, 3.62%. FT-IR (KBr), cm^{-1}: ν(OH) 3448wb, ν(N—H) 3130sb, ν(C=N) 1627s, ν(C=C$_{ring}$) 1581s, ν(C—O) 1319 m, ν(C—Cl) 678s, ν(C—Br) 585s. ^{1}H-NMR (100 MHz, DMSO-d_6, 25 °C, ppm): δ = 13.7 (s, 1H; O1H; Exchange with D_2O), 10.1 (s, 1H; O2H; Exchange with D_2O), 8.9 (s, 1H; C7), 7.9 (d, H; C5), 7.5 (dd, 2H; C1, C3), 7.3 (dd, H; C9), 6.9 (dd, 2H; C2, C12). UV/Vis (DMSO), λ_{max}, nm (log(ε), L mol^{-1} cm^{-1}): 286(4.03), 368(4.14), 438(3.67).

2.3. Preparation of the complexes

A mixture of H_2L (0.03 g, 0.1 mmol) in the appropriate solvent (methanol, ethanol and 2-butanol for **1**, **2** and **3** respectively) was mixed with [VO(acac)$_2$] (0.03 g, 0.1 mmol) and then was heated at 100 °C for 1 h. Crystals suitable for crystallography were obtained after the solutions had stood two or 3 days at room temperature.

2.3.1. (4-Bromo-2-(((5-chloro-2-hydroxyphenyl)imino)methyl)phenolato)methanol-methoxido-oxido-vanadium(V) (1)

Plate, red. Yield: 0.028 g, 61%. m.p.: 236 °C. Molar conductance (10^{-3} M, DMSO) 31.0 Ω^{-1} cm^2 mol^{-1}. Anal. Calc. for $C_{15}H_{14}BrClNO_5V$ (454.57 g mol^{-1}): C, 39.63; H, 3.10; N, 3.08. Found: C, 39.86; H, 2.51; N, 3.45%. FT-IR (KBr), cm^{-1}: ν(OH) 3232 m, ν(C=N) 1604s, ν(C=C$_{ring}$) 1527s, ν(C—O) 1296 m, ν(V=O) 964s, ν(C—Cl) 709s, ν(C—Br) 617s. ^{1}H-NMR (100 MHz, DMSO-d_6, 25 °C, ppm): δ = 9.3 (s, 1H; C7), 8.5–6.4 (m, 6H; rings), 3.2 (s, 3H; C14), 2.8 (s, 3H; C15). UV/Vis (DMSO, λ_{max}, nm (log(ε), L mol^{-1} cm^{-1}): 272(4.72), 442(4.37).

2.3.2. Di-[(4-bromo-2-(((5-chloro-2-hydroxyphenyl)imino)methyl)phenolato)ethoxido-oxido-vanadium(V)] (2)

Plate, red. Yield: 0.039 g, 45%. m.p.: 200 °C. Molar conductance (10^{-3} M, DMSO) 43 Ω^{-1} cm^2 mol^{-1}. Anal. Calc. for $C_{30}H_{24}Br_2Cl_2N_2O_8V_2$ (873.12 g mol^{-1}): C, 41.27; H, 2.77; N, 3.21. Found: C, 41.57; H, 2.63; N, 3.42%. FT-IR (KBr), cm^{-1}: ν(C=N) 1604s, ν(C=C$_{ring}$) 1535s, ν(C—O) 1280s, ν(V=O) 972s, ν(C—Cl) 709s, ν(C—Br) 624s, ^{1}H-NMR (100 MHz, DMSO-d_6, 25 °C, ppm): δ = 9.3 (s, 1H; C9), 8.3–6.5 (m, 6H; rings), 3.2 (q, 6H; C14), 1.5 (t, 6H; C15). UV/Vis (DMSO, λ_{max}, nm (log(ε), L mol^{-1} cm^{-1}): 270(4.98), 394(4.50), 442(4.61).

2.3.3. 2-Butoxy(4-bromo-2-(((5-chloro-2-hydroxyphenyl)imino)methyl)phenolato)oxido-vanadium(V) (3)

Plate, red. Yield: 0.022 g, 48%. m.p.: 218 °C. Molar conductanc (10^{-3} M, DMSO) 35 Ω^{-1} cm^2 mol^{-1}. Anal. Calc. for $C_{17}H_{16}BrClNO_4V$ (464.61 g mol^{-1}): C, 43.95; H, 3.47; N, 3.01. Found: C, 43.61; H, 3.41; N, 3.11%. FT-IR (KBr), cm^{-1}: ν(C=N) 1604s, ν(C=C$_{ring}$) 1535s, ν(C—O) 1288s, ν(V=O) 972s, ν(C—Cl) 709s, ν(C—Br) 624s. ^{1}H-NMR (100 MHz, DMSO-d_6, 25 °C, ppm): δ = 9.3 (s, 1H; C7), 8.4–6.4 (m, 6H; rings), 2.2–0.8 (m, 9H; C14, C15, C16, C17). UV/Vis (DMSO, λ_{max}, nm (log(ε), L mol^{-1} cm^{-1}): 272(4.75), 422(4.44).

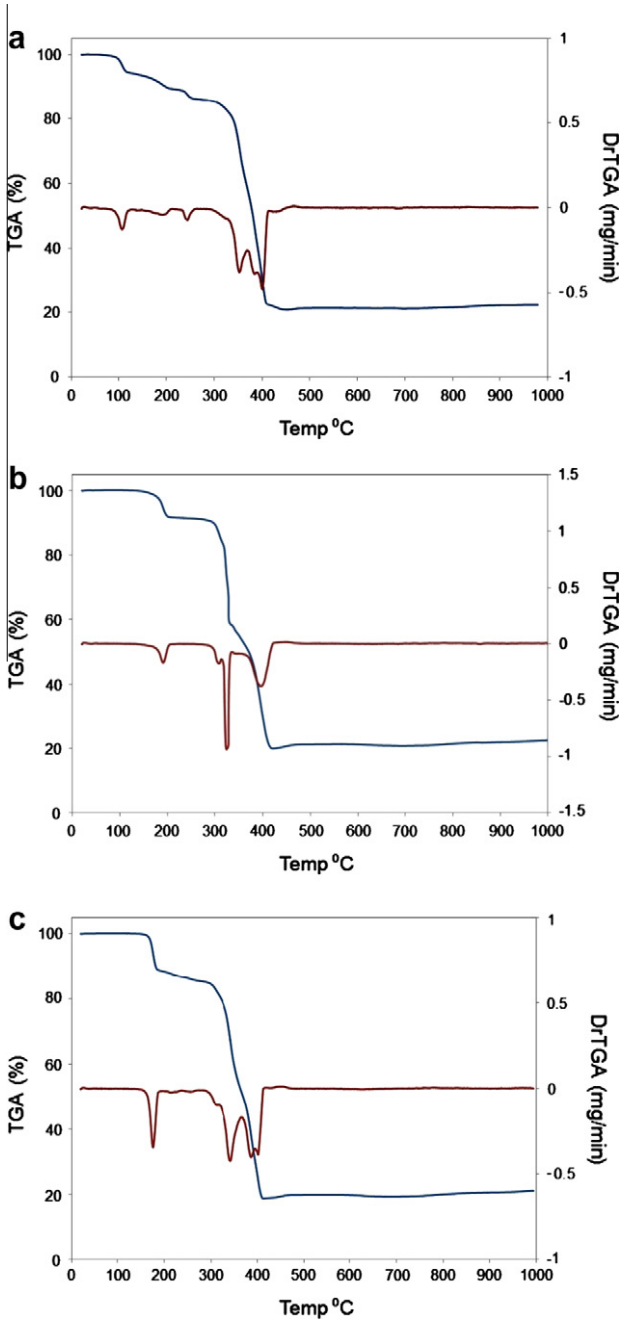

Fig. 1. TGA and derivative of TGA curves of **1** (a), **2** (b) and **3** (c).

2.4. Crystal structure determination

Crystals of the free ligand (H_2L) and **1**–**3** were mounted on a Cryoloop™ with Paratone™ oil and placed in the cold nitrogen stream provided by the low temperature attachment to the diffractometer. Full spheres of intensity data were collected using 3 sets of 400 frames, each of width 0.5° in ω, collected at φ = 0.00, 90.00 and 180.00° and 2 sets of 800 frames, each of width 0.45° in φ, collected at ω = −30.00 and 210.00° (H_2L and **1**) or 3 sets of 606 frames each of width 0.3° in ω collected at φ = 0, 120 and 240° (**2** and **3**). Inspection of *ca.* 1500 reflections chosen from the full data set for **2** with CELL_NOW [27] indicated that it consisted of two major components and one or two minor components. The raw intensity data were converted to F^2 values with SAINT [28] (for **2**, the crystal was treated as consisting of two components and the 2-component control file generated by CELL_NOW was used to generate a 2-component reflection file) with the same software executing a global refinement of unit cell parameters. Absorption corrections and merging of symmetry equivalent reflections were carried out with SADABS [29] (TWINABS [30] for **2**) and the structures solved by direct methods (SHELXS [31] for all but **2** which was solved with SHELXM [32]). The structures were refined by full-matrix, least-squares procedures (SHELXL [31]) and all other calculations were carried out with SHELXTL [33].

3. Results and discussion

The new Schiff base ligand (Scheme 1) as a zwitter-ion and three oxido-vanadium(V) complexes of it were prepared. The complexes are stable in air and were obtained as red crystals. They melt at temperatures considerably higher than the melting point of the ligand itself. The complexes are soluble in most solvents except water and *n*-hexane. The physical properties and elemental analyses of the ligand and its complexes are presented in the experimental section. Molar conductivity values of complexes are in the range 31–45 Ω^{-1} cm^2 mol^{-1} in DMSO, indicating non-electrolyte behaviors of them. All of the spectral and crystallography studies are in agreement with the proposed structures.

3.1. Spectral characterizations

Assignments of selected prominent IR bands in the 400–4000 cm^{-1} region for H_2L and its complexes are listed in the Experimental section. In the FT-IR spectrum of the ligand, bands observed in the regions 3448 and 3130 cm^{-1} are due to the O2H and NH vibrations. The absence of these frequencies in **1**–**3** indicates the azomethine nitrogen and phenolic oxygen atoms coordinate to the metal center. These data show also a red shift of the C=N vibration of the free ligand at 1627 cm^{-1} to a lower frequency at 1604 cm^{-1} in its complexes. This also indicates the coordination of the azomethine nitrogen to vanadium [34]. The bands at 972–964 cm^{-1} are assigned to ν(V=O) of the vanadyl moiety [35] while the ν(V—O) bands appearing at 540–563 cm^{-1} indicate the coordination of the alcohol and alkoxy ligands to vanadium [36]. The absence of the O2H band at ca. 3400 cm^{-1} [37] and the shift of the C—O band of H_2L (1319 cm^{-1}) to lower frequencies in the complexes (1280–1296 cm^{-1}) also supports coordination of the ligand to the metal through the phenolic oxygen [38]. The results confirm the presence of predominant *keto* form in solid state.

The electronic spectral data for the compounds in DMSO solution are presented in the Experimental section. Three bands at 286 nm, 368 nm and 438 nm are observed in the ligand. They can be attributed to $\pi \rightarrow \pi^*$ transitions of the phenyl ring and $\pi \rightarrow \pi^*$ and $n \rightarrow \pi^*$ of the azomethine moiety respectively [39]. The spectra of the complexes have similar features. The band at approximately 440 nm can be assigned to O(p) → V(d) charge transfer (LMCT) [40]. The presence of this CT band in the complexes is also strong evidence that the $(VO(OR))^{2+}$ is coordinated to oxygen of the ligand. The other bands are attributed to ring $\pi \rightarrow \pi^*$ intra-ligand transition [37]. The other L–L^* transition is covered by broad CT band.

The ^{1}H NMR spectrum of the ligand shows the presence of O1H at 13.7 ppm and O2H at 10.1 ppm that these shifts to low field indicate intramolecular hydrogen bonding between N···H—O1 and N···H—O2 respectively. Six-membered ring formation (**a** in Scheme 1) cause to more deshielding compare with five-membered ring in **b** (Scheme 1) [41]. The signal at 8.9 ppm is assigned to the methine proton while the protons of rings generate complex signals in the range 6.9 to 7.9 ppm. The ligand spectrum indicates existing only *enol* form in solution.

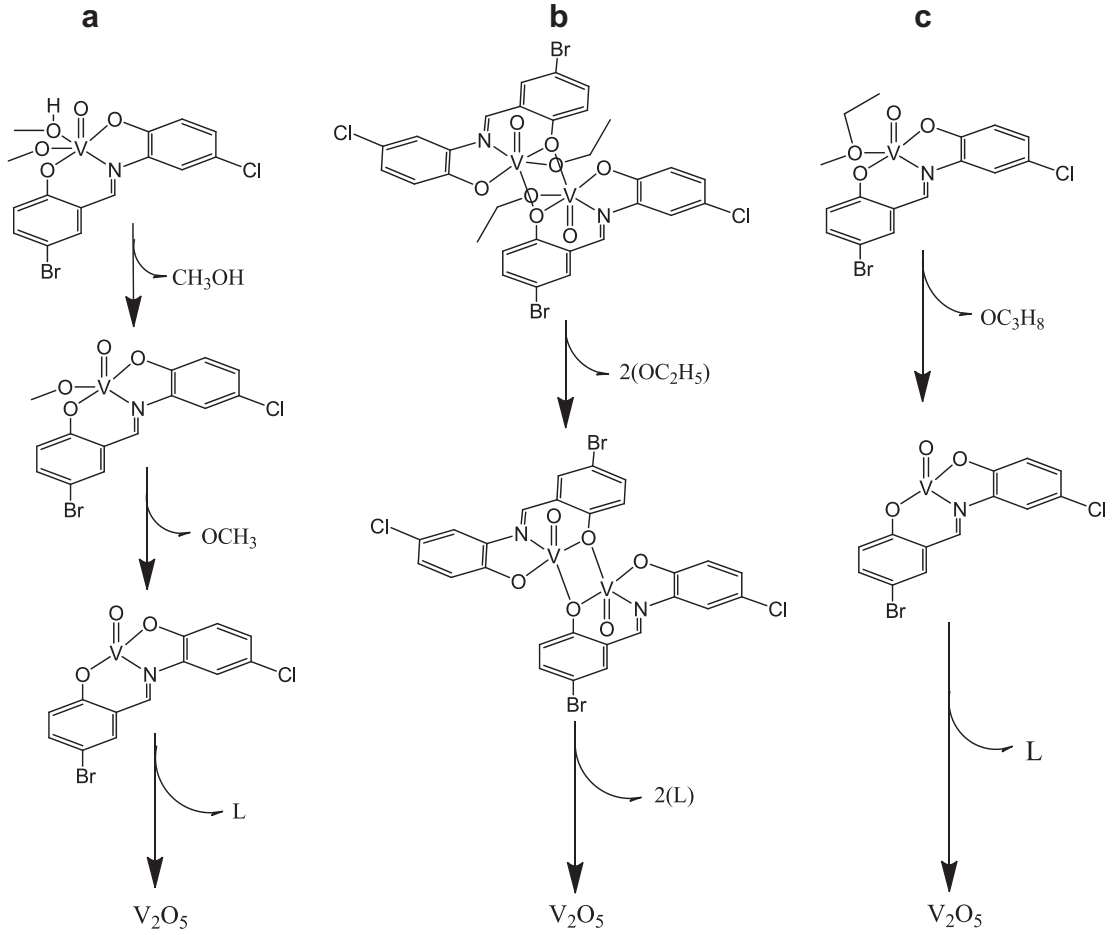

Scheme 2. Schematic diagram for decomposition steps of **1** (a), 2 (b) and 3 (c) (L = deporotonated form of H_2L).

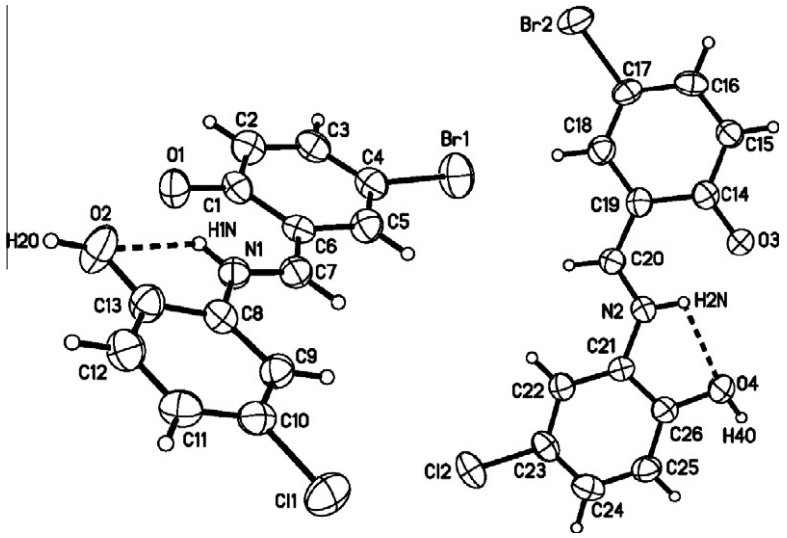

Fig. 2. Perspective view of the two independent molecules of H_2L showing the intramolecular hydrogen bonding. Displacement ellipsoids are drawn at the 50% level and hydrogen atoms are shown as spheres of arbitrary radius.

Upon coordination, the signals of phenolic protons disappeared showing that the oxygen atoms are now connected to the metal atom. In addition, the azomethine proton signal shifts about 0.3–0.5 ppm to lower field which is also consistent with coordination of the metal to the nitrogen. The protons of the coordinated methanol and of the methoxy ligand in complex **1** are assigned to singlets at 3.2 ppm and 2.8 ppm respectively. In compound **2** the CH_2 and CH_3 signals of the ethoxy ligand are detected at 3.2 ppm and

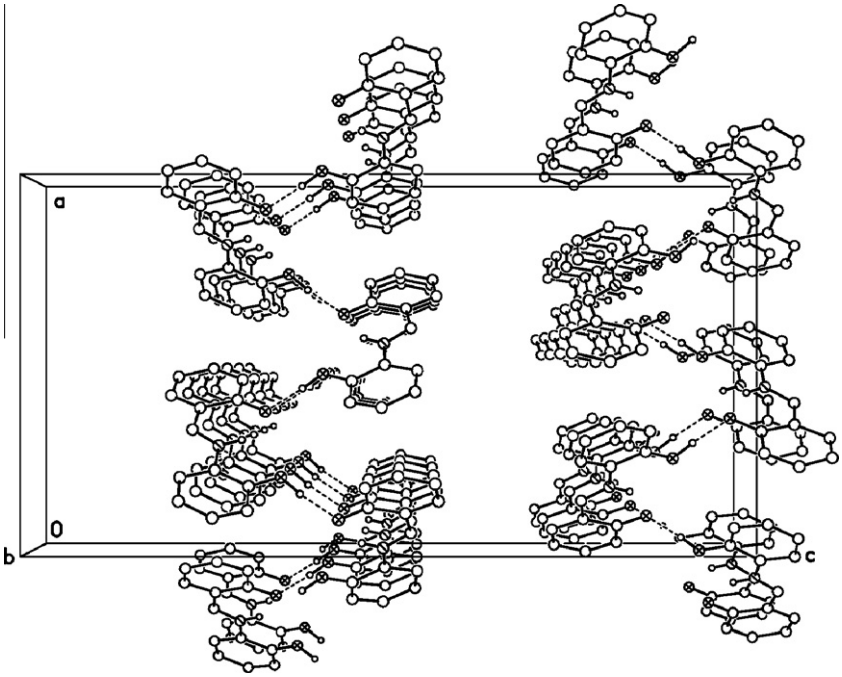

Fig. 3. Packing diagram for H_2L showing the intermolecular hydrogen bonding. Oxygen atoms are represented by cross-hatched circles and nitrogen atoms by shaded circles. Hydrogen atoms attached to carbon have been omitted.

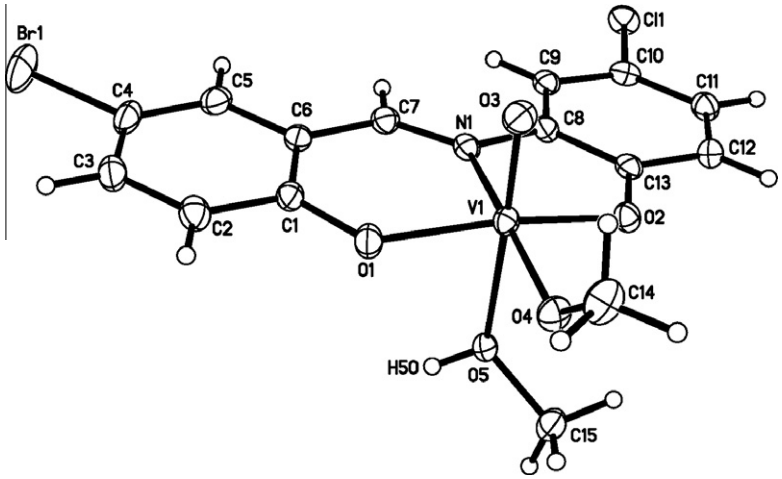

Fig. 4. Perspective view of **1** with displacement ellipsoids drawn at the 50% level and hydrogen atoms shown as spheres of arbitrary radius.

1.1 ppm respectively. Finally, the signals between 0.8 ppm and 2.2 ppm in **3** are assigned to the protons of the butoxy ligand.

3.2. Thermogravimetric analysis

The TG curve of pure complexes is given in Fig. 1 and decomposition steps for complexes is presented in Scheme 2. The thermogram of complex **1** shows it decomposing in three steps. In the first step, it loses 6.9% of its weight with the separation of a molecule of methanol at 107 °C and in the second step removal of the methoxy ligand occurs at 158–268 °C with a 7.3% weight loss and formation of VOL as a residue. The last TGA peak corresponds to decomposition of the residue to V_2O_5 at 293–419 °C (Fig. 1a). The other compounds decompose in two steps instead of three steps. The TG/DTG curves of compound **2** indicates a thermal decomposition at 190 °C corresponding to loss of two coordinated ethoxy groups with an 8.7% reduction in its weight and then at ca. 254–408 °C removal of two L ligands from the residue (74.38%) forming V_2O_5 (Fig. 1b). The TG curve for the **3** shows two mass losses up to 396 °C, the first at about 176 °C related to loss of the butoxy group with a 14.7% decrease in weight and a second mass loss over the 254–408 °C (65.8%) range which is due to L separation from the residue and complete conversion to V_2O_5 (Fig. 1c). The thermal stability of complexes is very similar with compound **1** showing slightly more thermal stability.

3.3. X-ray crystal structures

A perspective view of molecule **1** of the free ligand is presented in Fig. 2 while views of **1** and **3** appear in Figs. 4 and 6, respectively. A perspective view of the ordered dimer in **2** is given in Fig. 5, crystal data appear in Table 1 and pertinent bond distance and interatomic angles are listed in Table 2. The free ligand, H_2L, exists in the crystal as two independent molecules in the zwitterionic form

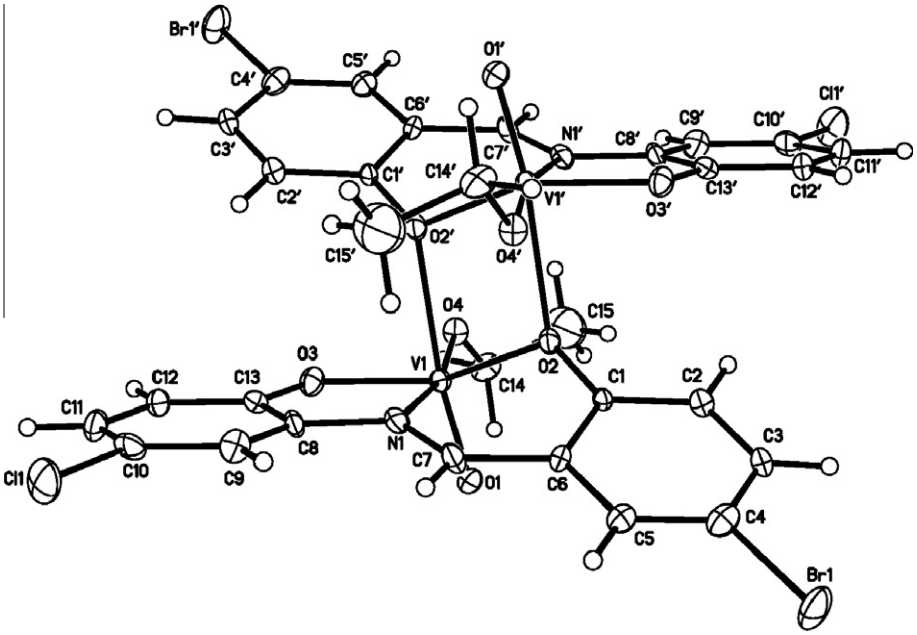

Fig. 5. Perspective view of the ordered dimer of **2** with displacement ellipsoids drawn at the 40% level and hydrogen atoms are shown as spheres of arbitrary radius.

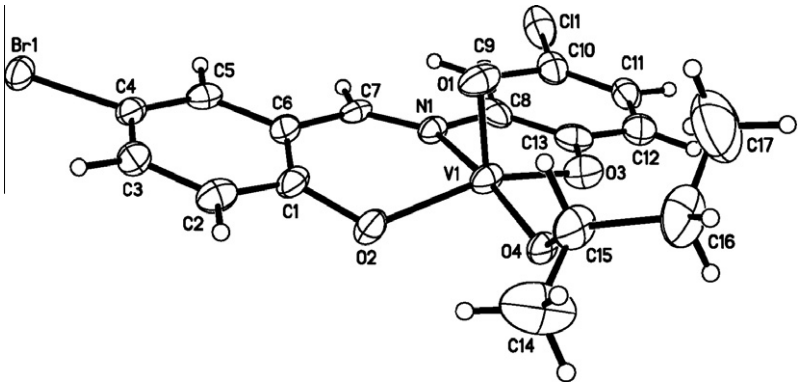

Fig. 6. Perspective view of **3** with displacement ellipsoids drawn at the 50% level and hydrogen atoms shown as spheres of arbitrary radius.

with the nitrogen protonated and the Br-substituted ring in the *keto* form. All hydrogen atoms were clearly present in a difference map calculated at the conclusion of the refinement of the non-hydrogen atoms, including that on nitrogen, conclusively demonstrating the zwitterionic character of H_2L. The molecule is held in an approximately planar conformation *via* intramolecular hydrogen bonding between the N—H group and the *ketonic* oxygen (H1N···O1 = 1.77 Å; N1—H1N···O1 = 148°. H2N···O3 = 1.82 Å; N2—H2N···O3 = 141°) while each independent molecule is associated *via* intermolecular hydrogen bonding between the phenolic hydrogen and the *ketonic* oxygen in the neighboring molecule (H2O—O3 (at $1.5 - x$, $1.5 + y$, $-0.5 + z$) = 1.60 Å; O2—H2O···O3 = 170°. H4O···O4 (at $1 - x$, $1 - y$, $0.5 + z$) = 1.64 Å; O4—H4O···O4 = 164°) to generate helical chains approximately parallel to the *a* axis (Fig. 3). The geometry and conformations of the two independent molecules are quite similar.

The structure of **1** consists of a vanadyl group in a distorted octahedral environment (Fig. 4) with the distortions primarily the results of the constraints of the tridentate ligand and the short V=O distance (Table 2). The remaining ligands are a methoxy group in the equatorial plane and an axial methanol molecule. The Schiff base ligand is slightly twisted as indicated by the angle between the planes of the two 6-membered rings of 3.0(1)°. The rms deviation of the equatorial atoms O1, O2, O4 and N1 from planar is 0.038 Å indicating significant distortion of the equatorial plane. A better indication of the distortion on the equatorial plane is obtained by considering the plane defined by the atoms C1, C7, N1, C8 and C13 of the ligand backbone from which the displacements of the metal and the ligating atoms are: V1, 0.293(3); O1, −0.094(3); O2, 0.03(3); O4, 0.064(5); N1, 0.030(1) Å. The relatively small displacement of the metal from the mean coordination plane is the result of the presence of the methanol in the axial position [42].

Complex **2** crystallizes as a dimer with crystallographically-imposed centrosymmetry (Fig. 5). Again, the metal atom resides in a distorted octahedral environment consisting of the donor atoms of the Schiff base ligand, the vanadyl oxygen, an ethoxy group and the oxygen atom (O2) on the Br-substituted ring of the ligand in the other half of the dimer. Similar unsymmetrical $\{V_2(\mu\text{–}O)_2\}$ moieties with V—O distances of 1.896(4)–1.940(4) and 2.285(3)–2.460(4) Å have been reported [43–47]. The sharing of O2 and its centrosymmetrically-related counterpart between the two metals in the dimer causes a much greater distortion of the equatorial plane than is the case in **1** as indicated by the ligand "twist" of

Table 1
Crystal data for complexes.

	H_2L	1	2	3
Empirical formula	$C_{13}H_9BrClNO_2$	$C_{15}H_{14}BrClNO_5V$	$C_{30}H_{24}Br_2Cl_2N_2O_8V_2$	$C_{17}H_{16}BrClNO_4V$
Formula weight	326.57	454.57	873.11	464.61
Temperature (K)	200(2)	100(2)	200(2)	100(2)
Wavelength (Å)	0.71073	0.71073	0.71073	0.71073
Crystal system	Orthorhombic	Monoclinic	Monoclinic	Monoclinic
Space group	$Pna2_1$	$P2_1/n$	C2/c	$P2_1/c$
Unit cell (Å, °)				
a	14.6624(9)	10.0199(6)	47.379(12)	8.5910(5)
b	6.0680(4)	9.8786(5)	16.768(4)	15.9263(10)
c	28.3638(17)	17.3460(9)	8.0258(18)	13.2200(8)
β		100.897(1)	98.209(5)	98.473(1)
V (Å^3)	2523.6(3)	1685.99(16)	6311(3)	1789.06(19)
Z	8	4	8	4
Dens. (calc, Mg/m^3)	1.719	1.791	1.838	1.725
Abs. coef. (mm^{-1})	3.461	3.141	3.348	2.959
F(000)	1296	904	3456	928
Crystal size (mm^3)	0.25 × 0.17 × 0.13	0.27 × 0.19 × 0.07	0.03 × 0.17 × 0.19	0.24 × 0.15 × 0.07
θ range (°)	2.78–27.71	2.19–29.08	1.29–27.54	2.02–28.51
Total refls.	39983	28943	13844	15465
Indep. refls.	5890 [R_{int} = 0.0388]	4367 [R_{int} = 0.0361]	7158 [R_{int} = 0.0786]	4228 [R_{int} = 0.0303]
Compl. (%) to θ_{full}(°)	99.8; 27.71	99.2; 28.50	99.7; 27.00	99.4; 27.35
Abs. corr.	Numerical	Numerical	Numerical	Numerical
Max. & min. trans.	0.6876 and 0.4487	0.8219 and 0.5834	0.9026 and 0.0.3902	0.8174 and 0.5840
Refinement method	Full-matrix least-squares on F^2	Full-matrix least-squares on F^2	Full-matrix least-squares on F^2	Full-matrix least-squares on F^2
Data/restraints/params	5890/1/325	4367/0/219	7158/302/577	4228/14/261
Goodness-of-fit on F^2	1.024	1.035	1.043	1.094
Final R indices [$I > 2\sigma(I)$]	R1 = 0.0321, wR2 = 0.0789	R1 = 0.0303, wR2 = 0.0756	R1 = 0.0842, wR2 = 0.2526	R1 = 0.0532, wR2 = 0.1254
R indices (all data)	R1 = 0.0396, wR2 = 0.0823	R1 = 0.0386, wR2 = 0.0798	R1 = 0.1377, wR2 = 0.2280	R1 = 0.0598, wR2 = 0.1291
Largest diff. peak, hole	0.351, −0.610 e Å^{-3}	0.878, −0.507 e Å^{-3}	0.914, −3.072 e Å^{-3}	2.611, −0.892 e Å^{-3}

Table 2
Vanadium coordination sphere (Å, °).

1		2[a]		3[b]	
V1—O1	1.8714(13)	V1—O2	1.919(4)	V1—O2	1.881(3)
V1—O2	1.9402(13)	V1—O3	1.893(4)	V1—O3	1.897(3)
V1—O3	1.5977(14)	V1—O1	1.583(4)	V1—O1	1.592(3)
V1—O4	1.7683(13)	V1—O4	1.763(4)	V1—O4	1.762(7)
V1—O5	2.2681(13)	V1—O2′	2.360(4)	V1···O2′	2.610(3)
V1—N1	2.1736(15)	V1—N1	2.172(5)	V1—N1	2.184(4)
O1—V1—O2	154.71(6)	O2—V1—O3	147.70(18)	O2—V1—O3	145.00(13)
O1—V1—O3	84.39(6)	O2—V1—O1	98.7(2)	O2—V1—O1	102.57(14)
O1—V1—O4	100.44(6)	O2—V1—O4	102.10(18)	O2—V1—O4	96.8(4)
O1—V1—O5	79.80(6)	O2—V1—O2′	72.09(17)		
O1—V1—N1	84.39(6)	O2—V1—N1	80.85(18)	O2—V1—N1	92.45(13)
O2—V1—O3	98.47(6)	O3—V1—O1	105.1(2)	O3—V1—O1	106.12(15)
O2—V1—O4	92.39(6)	O3—V1—O4	94.94(14)	O3—V1—O4	91.6(5)
O2—V1—O5	79.82(5)	O3—V1—O2′	82.74(16)		
O2—V1—N1	77.68(6)	O3—V1—N1	76.88(18)	O3—V1—N1	76.00(13)
O3—V1—O4	101.57(6)	O1—V1—O4	100.3(2)	O1—V1—O4	102.6(4)
O3—V1—O5	173.53(6)	O1—V1—O2′	170.52(18)		
O3—V1—N1	93.03(6)	O1—V1—N1	91.8(2)	O1—V1—N4	92.45(13)
O4—N1—O5	84.77(6)	O4—V1—O2′	84.15(17)		
O4—V1—N1	163.47(6)	O4—V1—N1	166.9(2)	O4—V1—N1	164.6(4)
O5—V1—N1	80.51(5)	O2′—V1—N1	84.68(17)		

[a] O2′ related to O2 by 1.5 − *x*, 0.5 − *y*, 2 − *z*.
[b] O2′ related to O2 by 2 − *x*, 2 − *y*, − *z*.

27.1(2)°. For this reason, it is not possible to define a reasonable equatorial plane from which to measure the distortion as was done for **1**. Also present in the unit cell are two more dimers at half-occupancy each and disordered about the 2-fold rotation axis. Because of this extensive disorder, the detailed structural parameters of these dimers are not described in detail but they appear to have distorted geometries very similar to that of the ordered dimer.

Unlike **1** and **2**, complex **3** is found as a mixture of two co-crystallized isomers in an 88:12 ratio. The major isomer has Br1 on the left side when viewed along the V1-N1 line while the other has Br1 on the right. This leads to an apparent disorder of Br1 and Cl1 as well as C7 and N1 and this model was refined subject to the constraint that the occupancies of the two sites for each atom sum to 1.0. A disorder in the *S*-butoxy group was also noted and was refined by the split-atom model. Complex **3** adopts what could be considered an intermediate conformation between those of **1** and **2** since the "twist" of the ligand is 7.2(2)°. Inspection of a packing diagram indicates that two molecules related by a center of symmetry show apair wise V1···O2′ interaction of 2.610(3) Å which, although longer than that in the unsymmetrical dimers noted above, is nevertheless shorter than the sum of the van der Waals radii (*ca.* 3.54 Å) and so is considered to be a weak attractive interaction. That this interaction is not stronger can be attributed to the bulk of the *S*-butoxy group which makes contacts with the other half of the dimer which are approximately equal to the sums of the corresponding van der Waals radii. For more clarity the comparison of bond distances between free and coordinated Schiff base ligand are given in Table 3.

Table 3
Comparison of bond distances (Å) between free and coordinated Schiff base ligand.

	H_2L (avg.)	1	2	3
O1—C1	1.291(4)	1.323(2)	1.357(7)[a]	1.350(9)
C1—C6	1.432(6)	1.414(3)	1.410(8)	1.401(6)
C6—C7	1.416(4)	1.445(3)	1.463(8)	1.466(6)
C7—N1	1.300(4)	1.287(2)	1.291(8)	1.280(5)
N1—C8	1.408(4)	1.426(2)	1.421(7)	1.421(5)
C8—C13	1.407(6)	1.403(2)	1.394(8)	1.390(6)
C13—O2	1.350(4)	1.339(2)	1.333(7)[b]	1.341(5)

[a] C1—O2.
[b] C13—O3.

This five-coordinate geometry in **3** can distinguish as an intermediate between a trigonal–bipyramidal (TBPY) and square-pyramidal (SPY) geometry. Addison et al. have introduced the parameter τ (index of trigonality) and used it for qualification assigned the

five-coordinated complex between TBPY and SPY geometry. The parameter $\tau = \beta - \alpha/60$, where α and β are the two largest angles, belongs to the vanadium atom. An ideal square pyramid will have $\beta = 180^\circ$ and $\alpha = 180^\circ$ and therefore $\tau = 0\%$, but an ideal trigonal–bipyramidal structure will have $\beta = 180^\circ$ and $\alpha = 120^\circ$ and therefore $\tau = 100\%$. This τ value for this complex is obtained *ca.* 5.8% indicating complex has a near square-pyramidal geometry [48].

4. Conclusions

In this study, we present the synthesis and characterization of the new Schiff base ligand 4-Bromo-2-(((5-chloro-2hydroxyphenyl)imino)methyl)phenol (H_2L) and its three oxido-vanadium(V) complexes. The spectral studies are in agreement with proposed structure of all synthesized compounds. Based upon FT-IR, ^{1}H NMR and X-ray analyses, the *enol* and *keto* forms are predominated in solution and solid state respectively. The variation in structure type from a monomeric complex with an alcohol ligand for **1** to a strongly bound dimer in **2** and a very weak dimer in **3** can be attributed in large part to the alcohol solvent in which the synthesis was performed. Thus, with the small and strongly coordinating methanol molecule the methanol solvated monomer is formed while with the more weakly coordinating ethanol or 2-butanol, dimer formation is favored to fill the sixth coordination position about the metal. As noted above, the strength of the interaction in the dimer appears to depend on the bulk of the alkoxy ligand. The TGA decomposition to alcohol and alkoxy molecules in first step and finally remain V_2O_5 as a residue.

Supplementary data

CCDC 871631–871634 contain the supplementary crystallographic data for H_2L and **1–3**. These data can be obtained free of charge via http://www.ccdc.cam.ac.uk/conts/retrieving.html, or from the Cambridge Crystallographic Data Centre, 12 Union Road, Cambridge CB2 1EZ, UK; fax: +44 1223 336 033; or e-mail: deposit@ccdc.cam.ac.uk.

Acknowledgements

We would like to thank the Tulane University Chemistry Department for support of the Tulane Crystallography Laboratory. R.T. and A.A. Gratefully acknowledge the financial support provided for this work by the Ferdowsi University of Mashhad and Payame Noor University (PNU).

References

[1] M.R. Maurya, A. Kumar, J. Costa Pessoa, Coord. Chem. Rev. 255 (2011) 2315.
[2] K.C. Gupta, A.K. Sutar, C.C. Lin, Coord. Chem. Rev. 253 (2009) 1926.
[3] J.A.L. da Silva, J.J.R.F. da Silva, A.J.L. Pombeiro, Coord. Chem. Rev. 255 (2011) 2232.
[4] R.R. Eady, Coord. Chem. Rev. 237 (2003) 23.
[5] D. Rehder, G. Santoni, G.M. Licini, C. Schulzke, B. Meier, Coord. Chem. Rev. 237 (2003) 53.
[6] G.R. Willsky, A.B. Goldfine, P.J. Kostyniak, J.H. McNeill, L.Q. Yang, H.R. Khan, D.C. Crans, J. Inorg. Biochem. 85 (2001) 33.
[7] T. Kiss, T. Jakusch, D. Hollender, Á. Dörnyei, É.A. Enyedy, J.C. Pessoa, H. Sakurai, A. Sanz-Medel, Coord. Chem. Rev. 252 (2008) 1153.
[8] B. Mukherjee, B. Patra, S. Mahapatra, P. Banerjee, A. Tiwari, M. Chatterjee, Toxicol. Lett. 150 (2004) 135.
[9] A. Bishayee, A. Waghray, M.A. Patel, M. Chatterjee, Cancer Lett. 294 (2010) 1.
[10] Z.H. Chohan, S.H. Sumrra, M.H. Youssoufi, T.B. Hadda, Eur. J. Med. Chem. 45 (2010) 2739.
[11] K.H. Thompson, J.H. McNeill, C. Orvig, Chem. Rev. 99 (1999) 2561.
[12] T.G.F. Hudson, Vanadium; Toxicology and Biological Significance, Elsevier, New York, 1996. p. 140.
[13] M.C. Cam, R.W. Brownsey, J.H. McNeill, Can. J. Physiol. Pharmacol. 78 (2000) 829.
[14] I.G. Fantus, G. Deragon, R. Lai, S. Tang, Mol. Cell. Biochem. 153 (1995) 103.
[15] J.H. McNeill, V.G. Yuen, S. Dai, C. Orvig, Mol. Cell. Biochem. 153 (1995) 175.
[16] P. Plitt, H. Pritzkow, R. Kramer, Dalton Trans. (2004) 2314.
[17] M.J. Clague, N.L. Keder, A. Butler, Inorg. Chem. 32 (1993) 4754.
[18] M. Bashirpoor, H. Schmidt, C. Schulzke, D. Rehder, Chem. Ber. 130 (1997) 651.
[19] M.R. Maurya, A. Kumar, M. Abid, A. Azam, Inorg. Chim. Acta 359 (2006) 2439.
[20] L.A. Tyler, M.M. Olmstead, P.K. Mascharak, Inorg. Chem. 40 (2001) 5408.
[21] G. Romanowski, M. Wera, Polyhedron 29 (2010) 2747.
[22] R.N. Patel, K.K. Shukla, A. Singh, M. Choudhary, U.K. Chauhan, S. Dwivedi, Inorg. Chim. Acta 362 (2009) 4891.
[23] B. Baruah, S. Das, A. Chakravorty, Inorg. Chem. 41 (2002) 4502.
[24] J. Qiao, L.D. Wang, L. Duan, Y. Li, D.Q. Zhang, Y. Qiu, Inorg. Chem. 43 (2004) 5096.
[25] J. Zhang, Y. Lin, G. Jin, Organometallics 26 (2007) 4042.
[26] B. Nock, T. Maina, F. Tisato, M. Papadopoulos, C.P. Raptopoulou, A. Terzis, E. Chiotellis, Inorg. Chem. 38 (1999) 4197.
[27] G.M. Sheldrick, CELL_NOW, University of Göttingen, Germany, 2008.
[28] SAINT, Bruker-AXS, Madison, WI, 2009.
[29] G.M. Sheldrick, SADABS, University of Göttingen, Germany, 2009.
[30] G.M. Sheldrick, TWINABS, University of Göttingen, Germany, 2009.
[31] G.M. Sheldrick, Acta Cryst. A64 (2008) 112.
[32] G.M. Sheldrick, XM, University of Göttingen, Germany, 2004.
[33] SHELXTL, Bruker-AXS, Madison, WI, 2008.
[34] M. Ebel, D. Rehder, Inorg. Chem. 45 (2006) 7083.
[35] G.D. Triantafillou, E.I. Tolis, A. Terzis, Y. Deligiannakis, C.P. Raptopoulou, M.P. Sigalas, T.A. Kabanos, Inorg. Chem. 43 (2004) 79.
[36] H. Mimoun, M. Mignard, P. Brechot, L. Saussine, J. Am. Chem. Soc. 108 (1986) 3711.
[37] H.H. Monfared, S. Alavi, R. Bikas, M. Vahedpour, P. Mayer, Polyhedron 29 (2010) 3355.
[38] C. Pettinari, F. Marchetti, R. Pettinari, D. Martini, A. Drozdov, S. Troyanov, Inorg. Chim. Acta 325 (2001) 103.
[39] S.M. El-Medani, O.A.M. Ali, R.M. Ramadan, J. Mol. Struct. 738 (2005) 171.
[40] R. Dinda, P. Sengupta, S. Ghosh, T.C.W. Mak, Inorg. Chem. 41 (2002) 1684.
[41] O. Gungor, P. Gurkan, Spectrochim. Acta Part A Mol. Biomol. Spectrosc. 77 (2010) 304.
[42] Y.A. Simonov, M.A. Yampolskaya, S.G. Shova, V.K. Belskii, N.V. Gerbeleu, Dokl. Akad. Nauk SSSR 282 (1985) 895.
[43] G. Asgedom, A. Sreedhara, J. Kivikoski, J. Valkonen, E. Kolehmainen, C.P. Rao, Inorg. Chem. 35 (1996) 5674.
[44] S. Stucky, U. Heinz, H. Hegetschweiler, Monogr. Ser. Int. Conf. Coord. Chem. 8 (2007) 91.
[45] H. Hefele, E. Uhlemann, F. Weller, Z. Naturforsch., B: Chem. Sci. 52 (1997) 693.
[46] W.R. Browne, A.G.J. Ligtenbarg, J.W. de Boer, T.A. van den Berg, M. Lutz, A.L. Spek, F. Hartl, R. Hage, B.L. Feringa, Inorg. Chem. 45 (2006) 2903.
[47] W. Priebsch, D. Rehder, Inorg. Chem. 29 (1990) 3013.
[48] A. Addison, T. Rao, J. Reedjik, J. Van Rijn, J. Chem. Soc. Dalton Trans. (1984) 1349.